

Friction Anomalies at First-Order Transition Spinodals: 1T-TaS₂

Emanuele Panizon¹, Torben Marx⁴, Dirk Dietzel⁴, Franco Pellegrini¹,

Giuseppe E. Santoro^{1,2,3}, Andre Schirmeisen^{4,*} and Erio Tosatti^{1,2,3†}

¹*International School for Advanced Studies (SISSA), Via Bonomea 265, 34136 Trieste, Italy*

²*CNR-IOM Democritos National Laboratory, Via Bonomea 265, 34136 Trieste, Italy*

³*The Abdus Salam International Centre for Theoretical Physics (ICTP),*

Strada Costiera 11, 34151 Trieste, Italy and

⁴*Institute of Applied Physics, Justus-Liebig-University Giessen,*

Heinrich-Buff-Ring 16, 35392 Giessen, Germany

Revealing phase transitions of solids through mechanical anomalies in the friction of nanotips sliding on their surfaces is an unconventional and instructive tool for continuous transitions, unexplored for first-order ones. Owing to slow nucleation, first-order structural transformations generally do not occur at the precise crossing of free energies, but hysteretically, near the spinodal temperatures where, below and above the thermodynamic transition temperature, one or the other metastable free energy branches terminates. The spinodal transformation, a collective one-shot event with no heat capacity anomaly, is easy to trigger by a weak external perturbations. Here we propose that even the gossamer mechanical action of an AFM tip may locally act as a surface trigger, narrowly preempting the spontaneous spinodal transformation, and making it observable as a nanofrictional anomaly. Confirming this expectation, the CCDW-NCCDW first-order transition of the important layer compound 1T-TaS₂ is shown to provide a demonstration of this effect.

INTRODUCTION

The development of fresh theoretical and experimental tools aimed at revealing and understanding solid state phase transitions through their surface nanomechanical and nanofrictional effects is an ongoing unconventional, yet very useful approach. Friction of nanosized tips on dry solid surfaces has been proposed to represent what one might term “Braille spectroscopy” – reading the physics underneath by touching [1]. For second-order, continuous phase transitions, a notable example has been the detection of displacive structural transformations as reflected by AFM dissipation anomalies caused by critical fluctuations, predicted [2] and observed in noncontact friction on SrTiO₃ [3]. Another non-structural example is the drop of electronic friction, observed upon cooling a metal below the superconducting T_c in correspondence to the opening of the BCS gap [4]. The injection of a 2π phase slip in the local order parameter of an incommensurate phase is an additional interesting event that can be triggered by an AFM tip.[5]

A vast majority of solid state structural and electronic phase transitions is, however, of discontinuous, first-order type. Should one expect

a frictional anomaly at the surface of a solid which undergoes a first-order structural transition? Lacking critical fluctuations, that frictional signature might it not just consist of some unpredictable and unremarkable jump? This scenario is, we propose, unduly pessimistic, countering that not one but two frictional anomalies are to be expected at a first order transition. They should occur at the hysteresis end-point temperatures, where both heating and cooling transformations are close in character to spinodal – the point where the dissolution of a metastable state takes place. At these two temperatures, on both sides of the thermodynamic transition temperature, an Atomic Force Microscope/Friction Force Microscope (AFM/FFM) dissipation peak is to be expected as the tip moves on, sweeping in the course of time newer and newer surface areas where the near-spinodal transformation can be “harvested”. These predictions are first argued theoretically and then demonstrated experimentally in the important layer compound 1T-TaS₂.

MEAN-FIELD THEORETICAL MODEL

Beginning with theory, we adopt the simplest mean-field Landau-Ginzburg-Wilson [6] or Cahn-

Allen [7] approach, which works reasonably well for many structural transitions. Assume the schematic model bulk solid free energy density

$$f[\Psi] = -\frac{r}{2}\Psi^2(\rho) + \frac{u}{4}\Psi^4(\rho) + \frac{J}{2}(\nabla\Psi)^2 + h(\rho)\Psi(\rho), \quad (1)$$

(where r , u , J are positive parameters) governing the evolution of a generic, non-conserved real order parameter Ψ supposed to represent collectively all mechanically relevant thermodynamic variables, as a function of spatial coordinate ρ (in this schematic outline, we provisionally ignore the distinction between surface and bulk). The external field h includes here a uniform term describing the free energy imbalance between the two minima at negative and positive Ψ (h thus represents here the temperature deviation from the first-order thermodynamic transition point) plus a localized mechanical perturbation representing the tip which, when moving in the course of time, will undergo mechanical dissipation, observable as friction. In the spatially uniform, field-free case $(\nabla\Psi)^2 = 0$, $h = 0$, two equivalent free energy minima $F_0 = -r^2/4u$ occur at $\Psi_0^\pm = \pm\sqrt{r/u}$ identifying the two phases. A first order transition occurs between them when a growing uniform h causes Ψ to switch from initially positive to negative or viceversa. For the transition to occur near $h = 0$ nucleation is required, allowing thermal crossing of the large free energy barrier between the two nearly equivalent states. Nucleation is a generally slow process so that a $\Psi > 0$ metastable state often persists up to large positive fields h . Upon reversing the field, the $\Psi < 0$ state can similarly persist for negative h , giving rise to hysteresis. The maximum theoretical width of the hysteresis cycle is determined by the two *spinodal* points $h_s = \pm 2r^{3/2}/3^{3/2}u^{1/2}$, where the transformation must necessarily take place because at each of them the metastable free energy minimum disappears, as sketched in Fig.1(a). At the spinodal points $\Psi_s = \pm\sqrt{r/3u}$ and $f_s = (1/12)r^2/u$ the transformation occurs collectively rather than locally, as amply described in literature, reviewed in a different context in [8].

A spinodal point is associated with the collective dynamics of all macroscopic variables accompanying the first order transition including structure, volume, conductivity, etc. As that point is

approached, even a small perturbation can locally overcome the marginal free energy barrier and trigger a large-scale transformation from the metastable to the stable state, as pictured in Fig. 1(a). If that perturbation is provided by a sliding tip, the small but finite triggering work will show up as a frictional dissipation burst. As the tip moves on, it can convert newer and newer patches from metastable to stable, Fig. 1 (b). The pursuit of the frictional consequences of a first order transition close to its spinodal points is our goal.

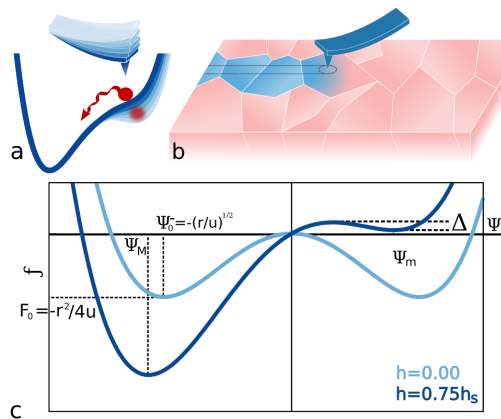


FIG. 1: a) Schematic representation of free energy behaviour versus order parameter near a spinodal point, and triggering action of an external tip; b) schematic of a sweeping tip on a solid with domains, triggering the local metastable-stable transformation and leaving behind a transformed trail; c) parameters of the free energy density near a spinodal point.

Starting with $\Psi > 0$, and turning up the uniform field (i.e., lowering the temperature approaching from above the real system spinodal temperature on cooling down) $h \rightarrow h_s$, we observe that $f[\Psi]$ is a local minimum – a metastable state – protected by a marginal barrier Δ which disappears at the spinodal point $h = h_s$, Fig. 1(c). Before that point is reached, in the metastable state, a weak static local perturbation $\delta h(\rho)$ imparts to the state variable Ψ a local modification, whose effect, initially small, grows as the spinodal point is approached. If moreover the perturbing agent, in our case the nano-tip, moves in space with velocity \mathbf{v} , so that $h_{\text{tip}}(\rho, t) = h_0(\rho - \mathbf{v}t)$, then it may or it may not succeed to locally trigger the spinodal transformation. If it does, then some mechanical work will be spent, and that expense will reflect in the form of a burst in the tip's mechanical dissipa-

tion.

Four different frictional regimes are crossed as a function of h (i.e., of temperature) – for example when evolving from a high temperature metastable state Ψ_m to a low temperature stable state Ψ_M on cooling. In regime (I), h is still far from the spinodal point h_s , the free energy barrier protecting the metastable state is substantial, the tip perturbation is too weak to push the system over it, and the tip friction is unaffected. In a second regime (II), the tip may succeed to “wet” its surrounding with a small converted nucleus Ψ_M of radius R_{tip} , yet still unable to overcome the nucleation barrier if $R_{\text{tip}} < R_c$, the effective “inhomogeneous” nucleation critical radius. Depending whether this nucleus does or does not reconvert back to Ψ_m as the tip moves on, there will or will not be frictional work. Assuming reconversion (for slow tip motion), the friction is again zero, because the transformed nucleus is carried along adiabatically by the tip. In regime (III), as h increases, the nucleation radius eventually gets smaller than the tip perturbation radius, $R_c < R_{\text{tip}}$. The system suddenly overcomes the barrier as in Fig. 1(a), thus provoking the irreversible transformation $\Psi_m \rightarrow \Psi_M$ extending in principle out to infinite distance – in practice, out to some macroscopically determined radius L defined by the sample quality, defects, and morphology. At this threshold temperature the mean tip frictional dissipation will suddenly jump from zero to finite, thereafter decreasing smoothly and eventually vanishing when the true spinodal point $h \rightarrow h_s$ is reached, and dissipation again disappears, regime (IV). Our model predicts the frictional dissipation burst in the shape shown Fig. 2, a behaviour which we now describe in our model before seeking an experimental demonstration.

Consider a configuration where, as in classical nucleation theory (CNT) the system is forced to evolve from $\Psi = \Psi_M$ at $\rho=0$, to $\Psi = \Psi_m$ at $\rho = \infty$. A trial function that shows this behaviour is constructed as $\Psi(\rho) = \Psi_m + (\Psi_M - \Psi_m)/2 \tanh((\rho - R_0)/\gamma)$, where R_0 is the radius of the droplet and γ its interface width. We consider the nucleation barrier $F[\rho; R_0, \gamma]$, which depends variationally on the two parameters R_0 and γ . Based on that we can numerically calculate the homogeneous nucleation radius R_c and

its corresponding barrier. Now add to $F[\rho]$ the tip perturbation $h_{\text{tip}}(\rho) = h_{\text{tip}}\Theta(\|\rho - \mathbf{x}_{\text{tip}}\| - R_{\text{tip}})$ whose effect is to lower the local barrier as sketched in Fig. 1(a). At $h = h_c$ the nucleation radius becomes smaller than the wetting radius $R_c < R_{\text{tip}}$, the local nucleation barrier disappears and the massive transformation is triggered. The tip will spend at that point the one-shot triggering work $W = F_0$. This work, as mentioned, is paid only once, because after conversion the stable phase Ψ_M extends macroscopically away, and the system becomes subsequently insensitive to the tip. It should be stressed here that, unlike second order transitions between equilibrium states, which take place reversibly as the temperature is cycled across the critical point, the spinodal transformation takes place only once as the spinodal point is first crossed (unless the system is, as it were, “recharged”). In a real system, however, the size of the transformed region is limited by defects to some average radius L determined by, e.g., grain boundaries, steps, etc., so that newer and newer metastable surface areas can be “harvested” in the course of time, as sketched in (Fig. 1(b)). The tip moving with velocity v will explore fresh untransformed metastable regions with a rate $\mu \sim v/L$, (Fig 1(c)) therefore dissipating a frictional power $P = W\mu = F_0v/L$, a quantity which is nonzero in the temperature range corresponding to $h_c < h < h_s$ as depicted in Fig. 2.

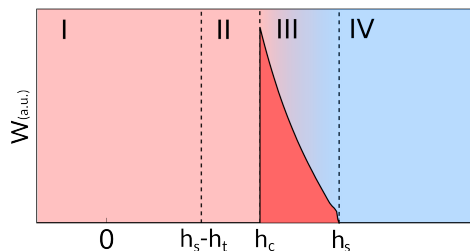


FIG. 2: Predicted tip dissipation W as a function of h (red area). In the cooling example, increasing h stands for decreasing temperature, and $h = h_s$ is the spinodal point. The sharp dissipation peak occurs at the threshold temperature where the tip perturbation succeeds in triggering the metastable state’s demise, thus preempting the spontaneous spinodal transformation before h_s is reached. The threshold h_c depends on details including the tip nature, radius, and load. In this figure the tip radius was $R_{\text{tip}} \sim 1.1\sqrt{r/u}$, other parameters were $u = 10$, $r = 10$ and $j = 1$. The regions I, II, III and IV are defined in text.

EXPERIMENTAL VERIFICATION IN 1T-TaS₂

Thus far the theory. To verify predictions in a well defined, physically interesting case we choose a thermally driven structural transition with an established hysteresis cycle between phases that do not differ too strongly from one another. Such is the case of the transitions in the celebrated layer compound 1T-TaS₂ between a low-temperature Commensurate Charge-Density-Wave (CCDW) $\sqrt{13} \times \sqrt{13}$ phase, [9, 10] believed to be Mott insulating [11, 12], and a Nearly Commensurate Charge-Density-Wave (NCCDW) phase, metallic and even superconducting under pressure [10]. This first-order transition takes place reproducibly in a single stage near $T_{NC} \sim 173$ K upon cooling, and in two stages, at $T_{CT} \sim 223$ K, $T_{TN} \sim 280$ K, upon heating. That very reproducible hysteresis pattern, partly reproduced from Ref. [10] in Fig. 3, suggests that T_{NC} and T_{CT} are, to a good approximation, spinodal points of 1T-TaS₂. That is strongly confirmed by very recent heat capacity data by Kratochvilova et al. [13], showing no anomaly at T_{NC} and T_{CT} , where at the same time large electrical and structural bulk transformations take place. A spinodal transformation occurs, upon temperature cycling $\pm \Delta T$, only once, thus averaging all internal energy effects to zero upon repeated passage.

It should also be mentioned that 1T-TaS₂ and its phases are and have been the subject of very intense studies over the last five years, in connection especially with transient or hidden metastable phases under high excitation [14–16] and/or in connection with unusual substrate, thickness, and disorder dependence of its phase transitions [17–20]. To begin with, we restrict here to bulk 1T-TaS₂ in equilibrium. Focusing for definiteness on the NCCDW \leftrightarrow CCDW transition upon cooling, and consider the phenomena which we might expect in AFM/FFM friction measurements as temperature crosses that transition. First, frictional heat dissipation into the substrate (phononic friction) could in principle differ in the two phases, because their structures, phonon spectra, mechanical compliances are, even if mildly, different – for example, the NCCDW structure possesses a network of “soliton”

defects, absent in the CCDW. Second, electronic friction due to creation of electron-hole pairs could be present in the NCCDW phase which is metallic, and not in the CCDW which is insulating. Both mechanisms do suggest a higher noncontact friction in the NCCDW phase above $T_{NC} \sim 173$ K than in the CCDW phase below that. Our experiment however measures hard contact friction, where these contribution turn out to be undetectable. The third, and central dissipation route described earlier is the main frictional feature which we observe near the spinodal points.

In our friction force microscopy experiments we used 1T-TaS₂-flakes with a size of approximately 4×4 mm² and a thickness before cleaving of about $50 \mu\text{m}$. To yield clean surface conditions, the samples were freshly cleaved directly before transfer to the UHV chamber of a commercial Omicron-VT-AFM/STM system. Inside the UHV chamber the samples were additionally heated to 100°C for 1h to remove residual adsorbates from the surface. To ensure that the sample is apt to detect the anticipated effects, we first used high resolution STM imaging to identify the most characteristic feature related to the NCCDW and CCDW, namely the $\sqrt{13} \times \sqrt{13}$ superstructure formed by 13 Ta-atoms arranged in a star shape around a central atom [9]. This superstructure is revealed in Fig. 3a, measured at 296K. At this temperature, the superstructure forms separate hexagonal domains, which coalesce during the phase transformation on cooling, leading to CCDW-1T-TaS₂ [10].

Subsequently we use high resolution friction force microscopy (FFM) for a first analysis of the sample with respect to tribological properties. Atomically resolved stick-slip is regularly observed and Fig. 3b shows an example, which was measured in the CCDW phase at 173K using a standard Si-cantilever (Nanosensors LFMR, normal force constant $k=0.2\text{N/m}$). Discerning the superstructure from the lateral force data in Fig. 3b is difficult but can be achieved by calculating the Fourier transform, where the superstructure leads to characteristic bright spots as shown in the inset of Fig. 3b.

In the first experimental run, which serves as a coarse-scale reference, we measure the temperature dependence of friction over a wide tempera-

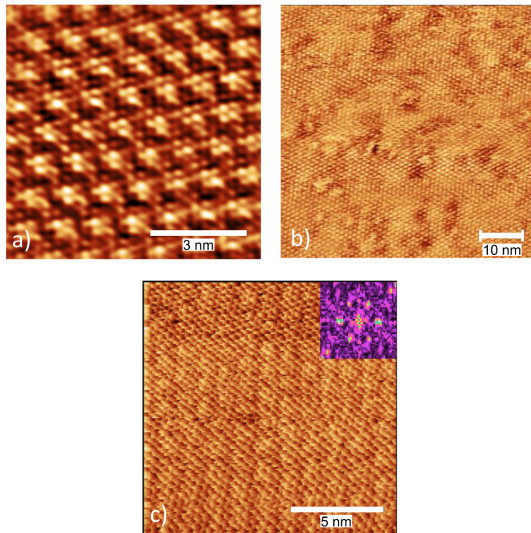


FIG. 3: a) Atomically resolved STM image ($8 \times 8 \text{ nm}^2$) of 1T-TaS₂ (296K, $I_T=1\text{nA}$, $U_T=5\text{mV}$). The $\sqrt{13} \times \sqrt{13}$ superstructure can clearly be identified and the experimental lattice constant of $a=1.1\text{nm}$ agrees with literature [21]. b) STM image ($60 \times 60 \text{ nm}^2$) recorded in the CCDW phase at 161K ($U_T=5\text{mV}$, $I_T=0.3\text{nA}$). The STM image reveals typical sizes of defect free regions of a few nm^2 . c) Friction force microscopy image obtained in the CCDW phase. A clear atomically resolved stick slip pattern is visible. The FFM image show only miniscule contrast for the superstructure, better visible in the Fourier transformation showing 6 bright spots (inset). Other frames, unlike this very perfect one, show defects and imperfections which set the effective length scale L discussed in text.

ture range from room temperature down to 160K. Fig. 4(bottom) shows that the friction remains constant within errors in the relevant range from 160K to 260K. In particular, there are no discontinuities across the transition temperatures $T_{NC} \sim 173 \pm 2 \text{ K}$ and $T_{CT} \sim 223 \text{ K}$ indicated by the dashed lines. Also there is no hysteresis between the cooling and heating cycles. One can see that incommensurability and metallization do not impact friction on this coarse scale. A much more detailed study is necessary to discern the influence of the hysteretic (spinodal) transformations, present in structure and in conductivity, on the tip friction.

We therefore focus on the friction signal in a narrow temperature window around the anticipated spinodal transition points. We use a specific experimental protocol to measure lateral forces while crossing the transitions. First, the NCCDW to CCDW transformation is analyzed

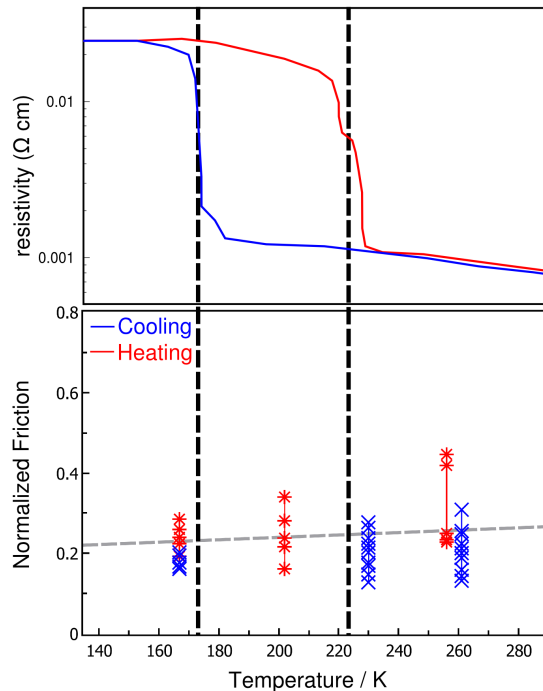


FIG. 4: Top) Bulk resistivity of 1T-TaS₂ versus temperature across the CCDW to NCCDW transitions, reproduced from Ref. [10]. Black dashed lined mark $T_{NC} \sim 173 \pm 2\text{K}$ and $T_{CT} \sim 223\text{K}$ on cooling and on heating respectively, transitions that are spinodal in character. Bottom) Coarse-scale temperature dependence of FFM friction relative to the average room temperature value, measured during cooling and heating. No direct correlation between friction and the change of electrical or of structurally commensurate or incommensurate characters is found across T_{NC} and T_{CT} within experimental error.

during cool down. For this the sample temperature was set to a constant value slightly above the transition point (appr. 195K). Once a stable sample temperature is established, continuous scanning of FFM images with a size of $50 \times 50 \text{ nm}^2$ at a normal force set-point of $F_N = 14 \text{ nN}$ and a scan speed of $v_{\text{scan}} = 250 \text{ nm/s}$ is started. Then the sample temperature is slowly reduced at a rate of appr. 0.2 K/min until the minimum temperature of 170K is reached, while the scanning is continuously running with the normal force feedback enabled. The temperature change induces a z-drift of the sample, and therefore only a small temperature window of about 10-20K is accessible with this method. Once the sample has been cooled down to the CCDW phase, the same procedure was used to analyse the transition from CCDW to NCCDW during heating. Here, 215K

was chosen as a starting point and the temperature was increased at a similar rate up to 225K, thereby spanning the full phase transition.

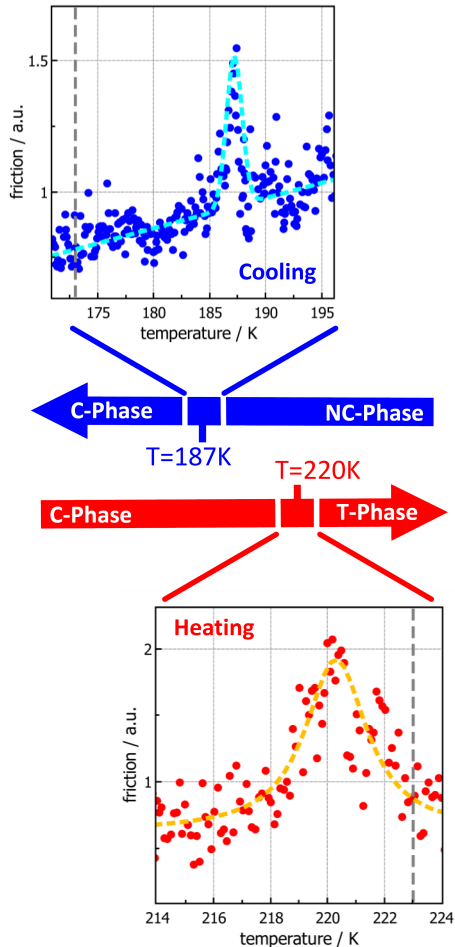


FIG. 5: Measured nanoscale friction on 1T-TaS₂ as a function of sample temperature across the two spinodal transformations. The cooling sequence (blue, upper part) shows the NCCDW to CCDW transformation, while the heating sequence (red, lower part) crosses the CCDW to trigonal NCCDW transition. There is no appreciable difference between stable and metastable state friction. Between the two, friction shows clear peaks at $186 \pm 2\text{K}$ and at $220 \pm 2\text{K}$ indicating the tip-induced preempting of the bulk spinodal transformations at T_{NC} and T_{CT} of 173K and 223K respectively (dashed lines).

For both cooling and heating sequences, the average friction force is calculated from each pair of lateral force images recorded for forward and backward scanning. Fig. 5 shows the resulting friction during cooling and heating as a function of the simultaneously recorded temperature. In both cases we see a clear peak in the average friction signal at the transition temperatures. The

peak height is approx 1.5 to 2 times higher than the average friction signal away from the transition point, while the peak width is about 2K to 5K. Results from further experiments reproduce these values. In contrast to published contact friction versus temperature results [22, 23], our result shows a very sharp and distinct transformation behavior, as is indeed expected from the spinodal theory.

Other details also fall qualitatively in place. The frictional peak on cooling occurs near 186 K, which is more than ten degrees higher than $173 \pm 2\text{K}$, the tip-free bulk transformation, assumed to coincide with the spinodal temperature. This is precisely what our theory predicts, the temperature difference corresponding to $h_c - h_s$, a quantity in principle dependent on details including tip size and applied load. Moreover, comparison of heating and cooling frictional peaks shows that the heating peak is lower in magnitude and deviates less from the bulk temperature $T_{CT} \sim 223\text{K}$. This is in agreement with a smaller difference expected in this case between Ψ_m and Ψ_M , reflecting the weaker character known for the transformation on heating relative to cooling.[24] The finite domain size L which limits the tip-triggered transformation could in 1T-TaS₂ be determined, besides the omnipresent defects shown in Fig. 3c, also by the recently discovered interplanar mosaic structure of this material.[25]

CONCLUSIONS

We have proposed theoretically a mechanism predicting frictional anomalies connected with spinodal points which end the hysteresis cycles of first order phase transitions. Direct experimental demonstration of the anomaly is provided by FFM nanofriction measured at the two transformations which occur upon cooling (173K) and upon heating (223K) of the NCCDW \leftrightarrow CCDW transition of layered 1T-TaS₂, transformations which we argue are to a good approximation spinodal in character. Near the spinodal temperature the free energy barrier protecting the metastable phase decreases enough that the small mechanical perturbation provided by the pressing and sliding tip is sufficient to locally trigger

the transformation, thus preempting its spontaneous occurrence. The frictional anomaly predicted is transient, but can nonetheless be measured in steady sliding as the tip explores newer and newer untransformed areas. These results show that nanoscale friction, easy to interpret as it is, is as sensitive as resistivity or structural tools such as X-rays, and unlike thermodynamic quantities like heat capacity that are totally insensitive when applied to spinodal points of first-order phase transitions. In the specific case of 1T-TaS₂, a possible interplay between the known electrical and structural characters of the transformations – characters which apparently do not impact the contact friction – and their spinodal nature, which we exploit here for the first time, will deserve renewed attention in the future. Of special interest appears to be for example the possibility to trigger tip-induced frictional transformations from hidden states [15], and/or in the ultrathin material, where the spinodal temperature is strongly thickness dependent [17, 18].

* E-mail: schirmeisen@ap.physik.uni-giessen.de

† E-mail: tosatti@sissa.it

- [1] A. Vanossi, N. Manini, M. Urbakh, S. Zapperi, and E. Tosatti, “Colloquium: Modeling friction: From nanoscale to mesoscale,” *Reviews of Modern Physics*, vol. 85, no. 2, p. 529, 2013.
- [2] A. Benassi, A. Vanossi, G. E. Santoro, and E. Tosatti, “Sliding over a phase transition,” *Physical review letters*, vol. 106, no. 25, p. 256102, 2011.
- [3] M. Kisiel, F. Pellegrini, G. Santoro, M. Samadashvili, R. Pawlak, A. Benassi, U. Gysin, R. Buzio, A. Gerbi, E. Meyer, *et al.*, “Noncontact atomic force microscope dissipation reveals a central peak of SrTiO₃ structural phase transition,” *Physical review letters*, vol. 115, no. 4, p. 046101, 2015.
- [4] M. Kisiel, E. Gneco, U. Gysin, L. Marot, S. Rast, and E. Meyer, “Suppression of electronic friction on Nb films in the superconducting state,” *Nature materials*, vol. 10, no. 2, p. 119, 2011.
- [5] M. Langer, M. Kisiel, R. Pawlak, F. Pellegrini, G. E. Santoro, R. Buzio, A. Gerbi, G. Balakrishnan, A. Baratoff, E. Tosatti, *et al.*, “Giant frictional dissipation peaks and charge-density-wave slips at the NbSe₂ surface,” *Nature Materials*, vol. 13, no. 2, p. 173, 2014.
- [6] J. S. Langer, “Theory of the condensation point,” *Annals of Physics*, vol. 41, pp. 108–157, 1967.
- [7] J. Cahn and S. Allen, “A microscopic theory for domain wall motion and its experimental verification in Fe-Al alloy domain growth kinetics,” *Le Journal de Physique Colloques*, vol. 38, no. C7, pp. C7–51, 1977.
- [8] K. Binder, “Theory of first-order phase transitions,” *Reports on progress in physics*, vol. 50, no. 7, p. 783, 1987.
- [9] J. A. Wilson, F. Di Salvo, and S. Mahajan, “Charge-density waves and superlattices in the metallic layered transition metal dichalcogenides,” *Advances in Physics*, vol. 24, no. 2, pp. 117–201, 1975.
- [10] B. Sipos, A. F. Kusmartseva, A. Akrap, H. Berger, L. Forró, and E. Tutis, “From mott state to superconductivity in 1T-TaS₂,” *Nature materials*, vol. 7, no. 12, p. 960, 2008.
- [11] E. Tosatti and P. Fazekas, “On the nature of the low-temperature phase of 1T-TaS₂,” *Le Journal de Physique Colloques*, vol. 37, no. C4, pp. C4–165, 1976.
- [12] P. Fazekas and E. Tosatti, “Electrical, structural and magnetic properties of pure and doped 1T-TaS₂,” *Philosophical Magazine B*, vol. 39, no. 3, pp. 229–244, 1979.
- [13] M. Kratochvilova, A. D. Hillier, A. R. Wildes, L. Wang, S.-W. Cheong, and J.-G. Park, “The low-temperature highly correlated quantum phase in the charge-density-TaS₂ compound,” *npj Quantum Materials*, vol. 2, no. 1, p. 42, 2017.
- [14] L. Perfetti, P. Loukakos, M. Lisowski, U. Bovensiepen, H. Berger, S. Biermann, P. Cornaglia, A. Georges, and M. Wolf, “Time evolution of the electronic structure of 1T-TaS₂ through the insulator-metal transition,” *Physical review letters*, vol. 97, p. 067402, 2006.
- [15] L. Stojchevska, I. Vaskivskyi, T. Mertelj, P. Kusar, D. Svetin, S. Brazovskii, and D. Mihailovic, “Ultrafast switching to a stable hidden quantum state in an electronic crystal,” *Science*, vol. 344, pp. 177–180, 2014.
- [16] C. Laulhe, T. Huber, G. Lantz, *et al.*, “Ultrafast formation of a charge density wave state in 1T-TaS₂: Observation at nanometer scales using time-resolved x-ray diffraction,” *Physical review letters*, vol. 118, p. 247401, 2017.
- [17] M. Yoshida, Y. Zhang, J. Ye, R. Suzuki, *et al.*, “Controlling charge-density-wave states in nanoscale crystals of 1T-TaS₂,” *Scientific Reports*, vol. 4, p. 7302, 2014.
- [18] M. Yoshida, R. Suzuki, Y. Zhang, M. Nakano, and Y. Iwasa, “Memristive phase switching in two-dimensional 1T-TaS₂ crystals,” *Science Advances*, vol. 1, no. 9, p. e1500606, 2015.
- [19] R. Hovden, A. Tsen, P. Liu, B. Savitzky, *et al.*, “Atomic lattice disorder in charge-density-wave phases of exfoliated dichalcogenides (1T-TaS₂),”

- Proceedings of the National Academy of Sciences of the United States of America*, vol. 113, no. 41, pp. 11420–11424, 2016.
- [20] R. Zhao, Y. Wang, D. Deng, X. Luo, *et al.*, “Tuning phase transitions in 1T-TaS₂ via the substrate,” *Nano Letters*, vol. 17, no. 6, pp. 3471–3477, 2017.
- [21] R. E. Thomson, B. Burk, A. Zettl, and J. Clarke, “Scanning tunneling microscopy of the charge-density-wave structure in 1T-TaS₂,” *Physical Review B*, vol. 49, pp. 16899–16916, June 1994.
- [22] L. Jansen, A. Schirmeisen, J. L. Hedrick, M. A. Lantz, A. Knoll, R. Cannara, and B. Gotsmann, “Nanoscale frictional dissipation into shear-stressed polymer relaxations,” *Physical review letters*, vol. 102, no. 23, p. 236101, 2009.
- [23] L. Jansen, M. A. Lantz, A. W. Knoll, A. Schirmeisen, and B. Gotsmann, “Frictional dissipation in a polymer bilayer system,” *Langmuir*, vol. 30, no. 6, pp. 1557–1565, 2014.
- [24] D. Guy, A. Ghorayeb, S. Bayliss, and R. Friend, “High pressure investigation of the CDW phase diagram of 1T-TaS₂,” in *Charge Density Waves in Solids*, pp. 80–83, Springer, 1985.
- [25] L. Ma, C. Ye, Y. Yu, X. Lu, *et al.*, “A metallic mosaic phase and the origin of mott-insulating state in 1T-TaS₂,” *Nature Communications*, vol. 7, p. 10956, 2016.

Work in Trieste was supported through ERC MODPHYSFRICT Contract 320796, also benefitted from COST Action MP1303. Financial support in Giessen was provided by the German Research Foundation (Project DI917/5-1) and in part by COST Action MP1303 and LaMa of JLU Giessen.